Received: 27 November 2022 | Revised: 15 August 2023 | Accepted: 21 August 2023

DOI: 10.1111/1755-0998.13863

MOLECULAR ECOLOGY RESOURCES WILEY

RESOURCE ARTICLE

High-quality genome of a pioneer mangrove *Laguncularia racemosa* explains its advantages for intertidal zone reforestation

Ranran Zhu[1] | Shao Shao[1] | Wei Xie[1] | Zixiao Guo[1] | Ziwen He[1] | Yulong Li[1,2] | Wenqing Wang[3] | Cairong Zhong[4] | Suhua Shi[1] | Shaohua Xu[1,2]

[1]State Key Laboratory of Biocontrol, Guangdong Key Laboratory of Plant Resources, School of Life Sciences, Southern Marine Science and Engineering Guangdong Laboratory (Zhuhai), Sun Yat-sen University, Guangzhou, China

[2]School of Ecology, Sun Yat-sen University, Shenzhen, China

[3]Key Laboratory of the Coastal and Wetland Ecosystems (Xiamen University), Ministry of Education, College of the Environment & Ecology, Xiamen University, Xiamen, China

[4]Hainan Academy of Forestry (Hainan Academy of Mangrove), Haikou, China

Correspondence
Shaohua Xu and Suhua Shi, State Key Laboratory of Biocontrol, Guangdong Key Laboratory of Plant Resources, School of Life Sciences, Southern Marine Science and Engineering Guangdong Laboratory (Zhuhai), Sun Yat-sen University, Guangzhou, China.
Email: xushh27@mail.sysu.edu.cn and lssssh@mail.sysu.edu.cn

Funding information
Guangdong Basic and Applied Basic Research Foundation, Grant/Award Number: 2020A1515110164 and 2022A1515010962; Innovation Group Project of Southern Marine Science and Engineering Guangdong Laboratory (Zhuhai), Grant/Award Number: 311021006; National Natural Science Foundation of China, Grant/Award Number: 31830005 and 32100176

Handling Editor: Alison Gonçalves Nazareno

Abstract

Ecological restoration of mangrove ecosystems that became susceptible to recent habitat perturbations is crucial for tropical coast conservation. The white mangrove *Laguncularia racemosa*, a pioneer species inhabiting intertidal environments of the Atlantic East Pacific (AEP) region, has been used for reforestation in China for decades. However, the molecular mechanisms underlying its fast growth and high adaptive potential remain unknown. Using PacBio single-molecule real-time sequencing, we completed a high-quality *L. racemosa* genome assembly covering 1105 Mb with scaffold N50 of 3.46 Mb. Genomic phylogeny shows that *L. racemosa* invaded intertidal zones during a period of global warming. Multi-level genomic convergence analyses between *L. racemosa* and three native dominant mangrove clades show that they experienced convergent changes in genes involved in nutrient absorption and high salinity tolerance. This may explain successful *L. racemosa* adaptation to stressful intertidal environments after introduction. Without recent whole-genome duplications or activated transposable elements, *L. racemosa* has retained many tandem gene duplications. Some of them are involved in auxin biosynthesis, intense light stress and cold stress response pathways, associated with *L. racemosa*'s ability to grow fast under high light or cold conditions when used for reforestation. In summary, our study identifies shared mechanisms of intertidal environmental adaptation and unique genetic changes underlying fast growth in mangrove-unfavourable conditions and sheds light on the molecular mechanisms of the white mangrove utility in ecological restoration.

KEYWORDS
adaptive evolution, convergent evolution, genome, reforestation, white mangrove

1 | INTRODUCTION

Mangrove ecosystems are found at tropical and subtropical land–ocean boundaries and play essential roles in ecology and economy by providing carbon sequestration, blue carbon storage, protection against coastal disasters and ecological system balance maintenance (Menéndez et al., 2020). However, mangrove ecosystems are vulnerable to global climate change and human activity (Goldberg et al., 2020; Guo et al., 2018). Mangrove forests, major components of the ecosystems, are critical habitats that act as nurseries for many coastal species but have declined globally by 20%–35% over the past 50 years, leading to severe ecological and economic consequences (Goldberg et al., 2020; Zhao et al., 2022). Therefore, mangrove ecosystem restoration is urgently needed.

Selecting suitable plants for restoration of mangrove ecosystems is fundamentally important. Reforestation requires species that can adapt well to the area of introduction and grow and reproduce quickly to establish a stable population in a short time (Paul et al., 2010). However, mangrove habitats are affected by many stressors such as saline seawater, hypoxia and nutrition deficiency (Giri et al., 2011). These environmental factors vary greatly because of tidal inundation, rainfall, soil type and topography. Therefore, mangrove species used for reforestation must tolerate the most extreme intertidal conditions. Furthermore, reforestation is usually conducted in mudflats and sometimes in high-latitude areas. Mudflats are exposed to high light intensity, while low temperatures at high latitudes are a major factor limiting mangrove distribution (Kao et al., 2004; Lang et al., 2022). Species used for reforestation must overcome these environmental factors.

Laguncularia racemosa (L.) Gaertn, known as the white mangrove, is one of the most successful species used for mangrove reforestation in China. It is a dominant pioneer mangrove in its endemic of the Atlantic-East Pacific (AEP). It is the only member of the monotypic genus *Laguncularia*, belonging to the family Combretaceae of the Order Myrtales. The mangrove genus *Lumnitzera*, naturally found in Indian-western Pacific (IWP), is proposed to be its closest relative (Tan et al., 2002). This mangrove clade and *Conocarpus erectus* are the only mangroves among the >500 Combretaceae species.

After its introduction to Hainan, China, in 1999, *L. racemosa* has exhibited faster growth and higher reproductive capacity than the Chinese native species (Figure 1a–c; Figure S1; Berger et al., 2006; Zhong et al., 2011). It also adapts well to the environments where it has been introduced and tolerates a wide range of stress conditions found in intertidal habitats. While sensitivity to salinity change varies among mangrove species, *L. racemosa* tolerates a wide range of salinity and nitrogen levels in both its original and new habitats (Rodríguez- Rodríguez et al., 2018; Zhong et al., 2011). *L. racemosa* also does well when planted on exposed mudflats or high latitudes with low temperatures, performing better than other mangrove reforestation species (Feng et al., 2021; Li et al., 2020). These abilities make *L. racemosa* a prime candidate for use in mangrove reforestation in varying conditions.

The outstanding reforestation characteristics mentioned above coupled with frequent human introductions lead to widespread

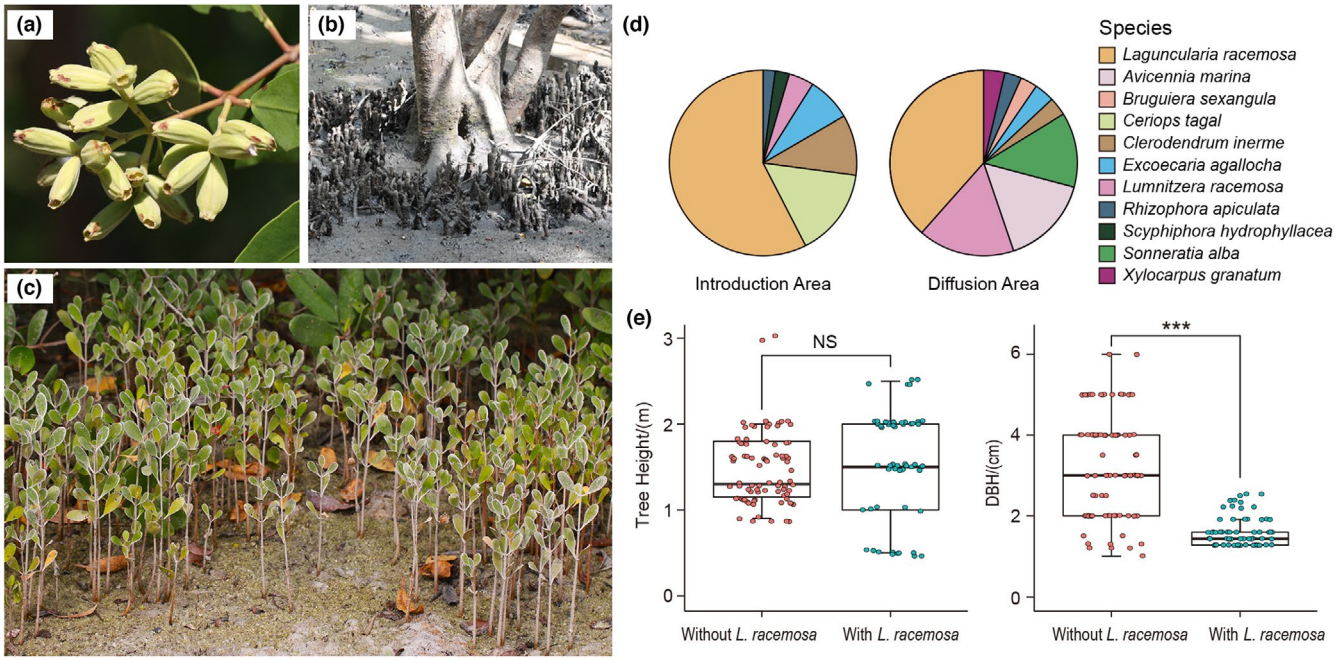

FIGURE 1 *Lagunculariaracemosa* plant images and field survey statistics. (a–c) Fruit, roots and a large group of *L. racemosa* seedlings. (d) Community importance value index of the mangrove forest in Yalong Bay (introduction area) and Tielu Harbour (diffusion area). (e) The height and diameter distribution of *Ceriops tagal* in communities with or without *L. racemosa* at Yalong Bay. *p*-values were estimated using the *t*-test. "NS" means not significantly different, asterisks represent *p*-values < .001.

presence of *L. racemosa* along the Southeast coast of China (Lang et al., 2022). However, these encouraging characteristics engender a risk that these species will become invasive. Field surveys show *L. racemosa* expanding in all areas of introduction, even becoming the main constituent of Hainan's secondary artificial mangrove forest (Fang et al., 2022; Zhong et al., 2011). Despite the abundance of ecological and physiological studies, we still do not understand the molecular mechanisms underlying these properties associated with mangrove reforestation in *L. racemosa*. This is a crucial missing piece that is needed if we are going to take full advantage of this species as a reforestation mangrove meanwhile preventing it from becoming invasive.

In this study, we sequenced and assembled a high-quality reference *L. racemosa* genome as part of a large worldwide mangrove genome sequencing project (He et al., 2022). With this de novo sequenced genome, we started by inferring its origin and divergence time from relatives. We then focused on the light this genome sequence can shed on mangrove reforestation and explored this issue in two aspects: (i) the genetic changes that contributed to *L. racemosa*'s tolerance to extremely high salinity and low nutrition levels; (ii) the molecular mechanisms underlying *L. racemosa*'s rapid growth, extreme light intensity and cold tolerance. The exploration of these issues would elucidate the advantages of *L. racemosa* as a reforestation species and provides a reference for assessing its invasive potential.

2 | MATERIALS AND METHODS

2.1 | Field survey

We performed a field survey of mangrove vegetation in the areas of Hainan Island where *L. racemosa* has been introduced (Yalong Bay, 18°22′ N, 109°61′ E) and spread (Tielu Harbour, 18°25′ N, 109°70′ E) on April 15, 2023. We sampled five 10 m by 10 m and one 5 m by 5 m (525 m^2 in total) of the initial introduction area and three 10 m by 10 m (300 m^2 in total) plots at location where *L. racemosa* has subsequently spread. We recorded the number of individuals of each species, stem diameter at breast height (DBH) and tree height within each plot. We then estimated relative density, relative frequency and relative dominance of each species according to Greig-Smith (1983). The importance value index (IVI) of each species was calculated as the arithmetic mean of the three parameters, reflecting the species' dominance in a community.

2.2 | Genome sequencing

We collected fresh *L. racemosa* leaf tissues from Dongzhai Harbor, to extract genomic DNA using the cetyl trimethyl ammonium bromide (CTAB) method (Doyle & Doyle, 1987). Genomic DNA was sequenced using the single-molecule real-time (SMRT) procedure on the PacBio sequel II platform (Pacific Biosciences). First, the extracted genomic DNA was sheared to ~25 kb on average and the fragments less than 7 kb were discarded using BluePipin (Sage Science). Then, the retained DNA fragments were used to construct an SMRTbell library using the Pacbio DNA template preparation kit (PacBio). Finally, SMRT sequencing was conducted on a PacBio Sequel II sequencing platform with the V3.0 sequencing reagent and SMRT Cell (8 M, V3).

We also performed DNA short-read sequencing to correct SMRT sequencing errors. Pair-end (PE) libraries (with 500 bp insert size) were constructed with the Illumina library preparation kit instructions and sequenced on the Illumina platform. To facilitate protein-coding gene prediction, we constructed RNA-seq libraries and sequenced them on the Illumina platform. RNA samples were extracted from leaf tissues using the TRIzol universal reagent. RNA-Seq libraries were constructed using a NEBNext Ultra RNA Library Prep Kit (Illumina) following the manufacturer's instructions and sequenced on an Illumina platform.

2.3 | De novo genome assembly

De novo assembly of the *L. racemosa* genome using PacBio long reads was conducted using FALCON with default parameters (Chin et al., 2016). The assembly was polished using Quiver (SMRT Analysis v2.3.0). To improve the assembly accuracy, we performed several rounds of iterative error correction based on Illumina short reads.

We further used Hi-C sequencing to improve genome assembly. To maintain DNA interactions, we fixed fresh leaf tissues using formaldehyde. The cross-linked DNA was digested with the MboI restriction endonuclease, and the resulting restriction fragment ends were biotinylated and ligated. Interaction among DNA fragments was used to construct a Hi-C library, which was then sequenced on the BGISEQ-500 platform. Raw reads were processed using SOAPnuke (V1.5.2) to remove adaptor sequences (match ratio >0.2) and low-quality reads (quality threshold <10, quality rate >0.1; parameters: −A 0.2 −l 10 −q 0.1; Chen et al., 2018). Clean Hi-C reads were then mapped *L. racemosa* assemblies following the HiC-Pro protocol to obtain valid reads and Hi-C interaction information (Servant et al., 2015). Hi-C maps were generated using Juicer (Durand et al., 2016). The scaffolds were roughly split by Juicebox and anchored to chromosomes as far as possible using 3D-DNA (Dudchenko et al., 2017; Robinson et al., 2018).

We used two widely used methods to evaluate genome assembly completeness (He et al., 2022; Wang et al., 2021; Xu et al., 2022). First, we mapped the clean short reads that used to correct SMRT sequencing errors to the genome assembly using BWA (V 0.7.17) (Li & Durbin, 2009). The high mapping rate would indicate high accuracy and completeness of the genome assembly. Second, we mapped the genomes to conserved eudicot core genes by benchmarking universal single-copy orthologues (eudicots_odb10 of BUSCO) using BUSCO (V5.0.0) (Manni et al., 2021).

2.4 | Genome annotation

We identified repetitive sequences using RepeatMasker with RepBase TE library (http://repeatmasker.org/). To ensure gene integrity

for subsequent analyses, we retained low complexity and simple repeats because they could be found in genes.

After repetitive sequences were masked, we predicted protein-coding genes with a combination of transcriptome-based, homology-based and ab initio methods. For transcriptome-based prediction, we mapped the clean RNA reads to the assembled genome using HISAT2 (V2.1.0) and assembled transcripts to gene models using Cufflinks (V2.2.1) (Kim et al., 2019; Trapnell et al., 2012). For homology-based prediction, we aligned the assembled genome to homologous proteins of several plants (*Arabidopsis thaliana*, *Eucalyptus grandis*, *Mimulus michiganensis*, *Oryza sativa* and *Sesamum indicum*) downloaded from NCBI or Phytozome (https://phytozome-next.jgi.doe.gov/). We then constructed gene structures based on the homology alignments using EXONERATE (V2.2.0) (Slater & Birney, 2005). We predicted coding genes ab initio using Augustus (V2.5.5) and GeneMark (V4.32) (Besemer et al., 2001; Stanke et al., 2006). All the gene models from the three methods were integrated using EvidenceModeler (EVM) into a non-redundant gene set (Haas et al., 2008).

Biological functions of the predicted genes were annotated by searching against the NCBI-NR (https://www.ncbi.nlm.nih.gov/), SwissProt (https://www.uniprot.org/) and TrEMBL in Uniprot (https://www.uniprot.org/) using BLASTP (*E*-value $< 10^{-5}$). We compared our gene models using eggNOG-mapper (V2.1.4) to the eggNOG (V5.0.2) database to obtain gene ontology (GO) and KEGG pathway annotations (Cantalapiedra et al., 2021; Huerta-Cepas et al., 2019). Transcription factors were identified using iTAK (v1.7) (Zheng et al., 2016).

2.5 | Repetitive element evolution

To explore whether repetitive elements have played roles in *L. racemosa* environmental adaptation, we calculated TE (transposable element) activity and inferred its influence on functional genes by measuring their distance since TEs can alter the activity of nearby genes (Muszewska et al., 2019). Therefore, we calculated the proportion of TEs that fall within a 1000 bp flanking region of genes in the *L. racemosa* genome and compared it with other mangroves and their inland relatives.

TE activity was then estimated by inferring LTR-RT (long terminal repeat retrotransposon) insertion times and the abundance of retro-transposed pseudogenes. We performed the identification of LTR-RTs using LTR_FINDER_parallel and LTRharvest that was implemented in genome tools based on the LTR-RT structure features (Gremme et al., 2013). LTR_retriever was then used to estimate the insertion time of LTRs based on sequence divergence between flanking long terminal repeat sequences (these sequences are identical at insertion time; Ou & Jiang, 2018). The LTR mutation rate was assumed to be twice the synonymous substitution rate in protein-coding genes (6.23×10^{-9} per bp per year) as calculated using PAML with the free-ratio model (Yang, 2007).

We also calculated the abundance of retro-transposed pseudogenes that are typically created by active TEs. Pseudogenes were first identified using PseudoPipe according to the pipeline of Xie et al. (2019) and the candidates were filtered using the following cut-offs: (1) amino acid sequence identity >40%; (2) BLAST *e*-value lower than 1e-10; (3) the pseudogenes cover 70% of the parent gene and (4) pseudogenes longer than 150 bp. The retro-transposed pseudogenes were then identified using a combination of three features: lacking introns, small flanking direct repeats and a 3′ polyadenine tail (Zhang et al., 2006).

2.6 | Phylogenetic analysis and divergence time estimation

We reconstructed the phylogenetic relationship between *L. racemosa* and additional closely related 11 species with available whole-genome sequences, including *Combretum micranthum*, *Conocarpus erectus*, *Lumnitzera racemosa* and *Lumnitzera littorea* from Combretaceae, *Punica granatum*, *Eucalyptus grandis* and *Melastoma dodecandrum* from other Myrtales families, *Arabidopsis thaliana* from Brassicales, *Rhizophora apiculata* and *Carallia pectinifolia* from Malpighiales and *Vitis vinifera* from Vitales (Hao et al., 2022; He et al., 2022; Luo et al., 2020; Myburg et al., 2014; Xie et al., 2022).

We inferred highly conserved single-copy genes using OrthoFinder and employed MUSCLE to align orthologous proteins and PAL2NAL to generate codon sequences against aligned protein sequences (Edgar, 2004; Emms & Kelly, 2019; Suyama et al., 2006). After discarding sequences shorter than 150 bp and removing gaps using Gblocks, high-confidence orthologous single-copy genes were used for phylogenetic tree reconstruction (Castresana, 2000). Based on 938 high-confidence orthologs, we reconstructed the phylogenetic tree using RAxML with the GTR + GAMMA model, 1000 bootstrap replicates and *V. vinifera* as the outgroup (Stamatakis, 2014).

Based on the phylogenetic relationship, we used MCMCTREE from the PAML package to estimate species divergence times (Yang, 2007). HKY85 + gamma nucleotide substitution and independent rates clock models were employed. Four known time points were set for calibration. The divergence of Combretaceae from their sibling family is between 93 and 112 Mya (million years ago) (Manchester & O'Leary, 2010). The common ancestor of *P. granatum* and *E. grandis* was placed at ~81 Mya (Grímsson et al., 2011). The common ancestor of *C. micranthum* and *C. erectus* was placed at ~53 Mya (Singh et al., 2010). The common ancestor of *R. apiculata* and *C. pectinifolia* was placed at ~47.8 Mya (Graham, 2006). We used Figtree for tree visualization (http://tree.bio.ed.ac.uk/software/figtree/).

To refine our estimates of *L. racemosa* origin, we reconstructed a higher resolution phylogenetic tree of Combretaceae using fewer genes, enabling us to include species without whole-genome sequences. *Macropteranthes kekwickii* from Australia were proposed to be *Laguncularia*'s close relatives. Therefore, three chloroplast gene sequences (*ndhf*, *psaA* and *rbcl*) of *M. kekwickii* and *Strephonema pseudocola* that are usually used as the Combretaceae outgroup were downloaded from the NCBI database and used for phylogenetic tree reconstruction. The orthologous sequences of

the three genes were found using BLAT from the complete chloroplast genome of *Combretum kraussii*, *Combretum indicum*, *Quisqualis littorea*, *Terminalia catappa*, *Anogeissus acuminata*, *Laguncularia racemosa*, *Lumnitzera racemosa*, *Combretum micranthum* and *Conocarpus erectus* (Table S4). We then employed MAFFT for sequence alignment and Gblocks to remove gaps (Katoh et al., 2002). Finally, we reconstructed the phylogenetic tree using RAxML with the GTR+GAMMA model, 1000 bootstrap replicates and *Strephonema pseudocola* as the outgroup.

2.7 | Genome synteny and whole-genome duplication

We tested for whole-genome duplication (WGD) events in *L. racemosa* by looking at the linear arrangement of homologous genes. We selected four additional Myrtales species (*C. erectus*, *Lumnitzera racemosa*, *E. grandis* and *P. granatum*) and *V. vinifera* for the analysis. Collinear genes and syntenic blocks within each genome and between genomes were inferred using MCScanX (Wang et al., 2012). We used identity ≥30% and *E*-value <1e-10 cut-offs to identify collinear homologous genes. Regions with ≥5 collinear homologous genes arranged in the same order were identified as syntenic blocks. Synonymous substitution rates (Ks) between homologous genes in syntenic blocks were calculated using KaKs_Calculator with the YN substitution model (Wang et al., 2010). Representative syntenic blocks were visualized using JCVI (Tang et al., 2008).

2.8 | Gene family evolution

We performed gene family clustering using the OrthoFinder pipeline. Based on the inferred gene family statistics, we quantified gene family copy number evolution using a random birth and death model in CAFE (Mendes et al., 2020). Expansions or contractions were considered significant if *p*-vValues <.01.

Ignoring WGD events, we explored the role of tandem (copies located next to each other) gene duplication. Specifically, tandem duplications were identified if two homologous genes (belonging to the same gene family) were in neighbouring regions of a chromosome (with fewer than 10 genes between them). We identified tandemly duplicated genes in eight plant genomes including two mangroves with recent WGD (*Avicennia marina* and *Rhizophora apiculata*), two mangroves without recent WGD (*Lumnitzera racemosa* and *C. erectus*), three non-mangroves (*C. micranthum*, *E. grandis* and *P. granatum*) and *L. racemosa*. We then performed gene functional annotations using eggNOG mapper (Cantalapiedra et al., 2021). Functional enrichment analyses, including GO and Kyoto Encyclopedia of Genes and Genomes (KEGG) enrichment, were complemented by ClusterProfiler (Yu et al., 2012).

We examined evolution of gene families involved in intense light tolerance, auxin biosynthesis and cold tolerance pathways. The genes involved in these pathways were identified by assigning *A. thaliana* homologues whose annotations were obtained from the TAIR10 database. The presence of tandem duplications in these pathways was examined in *L. racemosa* and the close relative *Lumnitzera racemosa*.

C-repeat-binding factors, key transcription factors in cold tolerance, experienced extensive tandem duplication in *L. racemosa* (see below). We examined these homologues' expression profiles under cold treatment using the transcriptome data of Zhang et al. (2023). Clean sequences from each sample were aligned to the reference genome using HISAT2 (v2.2.1) (Kim et al., 2019). Then, the generated SAM files were sorted and converted to BAM files using SAMtools (v1.9) (Li & Durbin, 2009). Transcriptome assembly was conducted using the simplified StringTie workflow (v2.1.4), which directly estimates and analyses the expression of a given transcript in the reference genome annotation file. Gene expression fold change was estimated using the R package 'DESeq2' (Anders & Huber, 2010). We further normalized gene expression using *z*-scores and used the R package 'pheatmap' to draw expression heatmaps.

2.9 | Detection of convergence in amino acid substitution and gene family evolution

After its introduction to China, *L. racemosa*, like widespread native mangrove species, adapted well to stressful and fluctuating intertidal environments. To explore the underlying mechanisms, we looked for molecular convergence between *L. racemosa* and three other phylogenetically independent native mangroves – *Avicennia marina*, *Rhizophora apiculata* and *Aegiceras corniculatum*. The three mangrove clades are widely distributed in the IWP region and have adapted well to varying intertidal conditions.

We first detected convergent amino acid (AA) substitutions using the CCS (Convergence at Conservative Sites) framework (Xu et al., 2017). For each independent mangrove species, we chose an inland relative with a good genome assembly as the ingroup control. In this case, we considered four mangrove:non-mangrove pairs: *Laguncularia racemosa* (Combretaceae, Myrtales) and *Punica granatum* (Lythraceae, Myrtales), *A. marina* (Acanthaceae, Lamiales) and *Mimulus guttatus* (Phrymaceae, Lamiales), *R. apiculata* (Rhizophoraceae, Malpighiales) and *Carallia pectinifolia* (Rhizophoraceae, Malpighiales), *A. corniculatum* (Primulaceae, Ericales) and Primula veris (Primulaceae, Ericales). *Oryza sativa* was used as the outgroup to infer the AA ancestral states. Phylogeny of the nine species was constructed according to the APG IV system.

Protein-coding genes were clustered into gene families using OrthoFinder. Within a gene family, we first identified orthologs in each mangrove:non-mangrove species pair by choosing the gene pair with the highest BLAST score. We then chose the *O. sativa* gene with the highest BLAST score to each gene pair as the outgroup. Candidates with sequence identity <50% or match lengths <40% were discarded. After aligning using MUSCLE and PAL2NAL, and filtering genes shorter than 50 AAs, we retained high-confidence orthologs (Edgar, 2004; Suyama et al., 2006).

We next identified conservative sites as those where the outgroup (O) shared the same AA with all four inland species (N), i.e., $O=N_1=N_2=N_3=N_4$. Conservative sites with all four mangrove species (M) sharing a different AA were considered to have experienced convergent substitutions in all four mangroves, i.e., $M_1=M_2=M_3=M_4\neq O$. As a control, we reversed the procedure and counted sites where all mangroves shared the ancestral state, but all non-mangroves had an alternative AA.

We also detected convergent gene copy number evolution in salt-response pathways. In addition to the four mangrove:non-mangrove pairs used above, we added three other inland species (*E. grandis*, *Populus trichocarpa* and *A. thaliana*) to control for the direction of expansion or reduction. Gene families in the salt-response pathway were annotated looking for orthologs of *A. thaliana* genes annotated as "response to salt stress" in the TAIR database. We used the average gene copy numbers among *E. grandis*, *P. trichocarpa* and *A. thaliana* as within-family controls. We considered gene copy number expansion in mangroves as convergently occurring only if (1) there were at least as many copies in mangroves as in the corresponding non-mangroves in all pairs; (2) the mangrove genomes contained more copies than the corresponding non-mangrove in at least three pairs and (3) mangroves had at least one more copy on average compared to the control group. The same criteria were applied to infer convergent expansion in non-mangroves. Similar criteria were used to infer convergent contraction.

3 | RESULTS

3.1 | The current reforestation practice using *Laguncularia racemosa*

We performed field surveys of mangrove vegetation on Hainan Island, the areas where *L. racemosa* was originally introduced (Yalong Bay) and subsequently expanded (Tielu Harbour). Mangrove forest in Yalong Bay was previously dominated by *Ceriops tagal* and experienced large-scale dieback caused by flooding in 2011. *L. racemosa*, therefore, was introduced for mangrove ecosystem restoration in 2012. After 10 years of growth, we observed that *L. racemosa* has established itself as the dominant species in both introduction and diffusion areas (Figure 1d).

To investigate the influence of *L. racemosa* on native mangroves specifically, we measured growth status of *Ceriops tagal*, a dominant native mangrove, in the community with or without introduced *L. racemosa*. *C. tagal* tree heights are similar on average in both communities but have a greater variance when *L. racemosa* is present (Figure 1e). Furthermore, *C. tagal* DBH levels are significantly lower in the community with *L. racemosa* (Figure 1e). The planted *L. racemosa* individuals grew to over 10 m and dominated the available sunlight where it was originally introduced. Fierce interspecific competition pushes other species to prioritize vertical growth over physical strength as a means of accessing sunlight. As a fast-growing mangrove, *L. racemosa* has exerted a significant influence on native mangrove life history and habit.

3.2 | High-quality *Laguncularia racemosa* genome

We sequenced the genome of *L. racemosa* by incorporating PacBio single-molecule real-time (SMRT) long reads and Illumina short reads. We obtained 124 Gb (approximately 108-fold coverage) of long reads with an average length of 12.45 Kb (Table S1; Figure S2). We also generated 143 Gb of short reads (approximately 124-fold coverage) with an average insertion size of 269 bp (Table S1).

We assembled the SMRT long reads into contigs and used the short reads to correct sequencing errors. The final *L. racemosa* assembly is 1105 Mb, covering 90.4% of the genome (1221 Mb, estimated using flow cytometry; Table 1; Figure S3). The longest scaffold is 17.58 Mb, and the N50 length is 3.46 Mb (Figure 2a). The GC content of the assembly is 34.54% and the estimated heterozygosity is ~1.96 sites per Kb. Genome validation revealed that 93.39% of short reads could be uniquely mapped to the genome assembly. We found complete structures for 96.0% of eudicot core genes listed in the BUSCO database in the genome assembly (Table S2). Together, these numbers indicate that our assembly is nearly complete and accurately reflects the *L. racemosa* genome.

Using a homology-based search using RepeatMasker (v4.1.1) and RepeatModeler (v2.0.1), we estimate that 66.96% (740 Mb) of the *L. racemosa* genome consists of repetitive sequences (Table S3). The most abundant repetitive sequences are LTR-RTs, accounting for 44.60% of the genome. With repetitive sequences masked, we predicted 21,070 protein-coding genes, and the completeness assessed by BUSCO is comparable to that of other high-quality genomes (Table 1; Table S2; Hu et al., 2022; Xu et al., 2022). There are 1724

TABLE 1 Statistics of *Laguncularia racemosa* genome assembly.

Assembly feature	Statistics
Genome size (Mb; flow cytometry)	1221
Total length (Mb)	1105
N50 (Mb)	3.46
Counts of N50	84
Counts of Contigs	6513
Longest (Mb)	17.58
Gene number	21,070
Annotated gene number	20,926
Average gene length (Kb)	6.1
TE content (%)	66.96
TE length (Mb)	740.07
Heterozygosity (sites/Kb)	1.96
GC content (%)	34.54
BUSCO completeness (%)	96

Abbreviation: GC, guanine/cytosine; TE, transposable element.

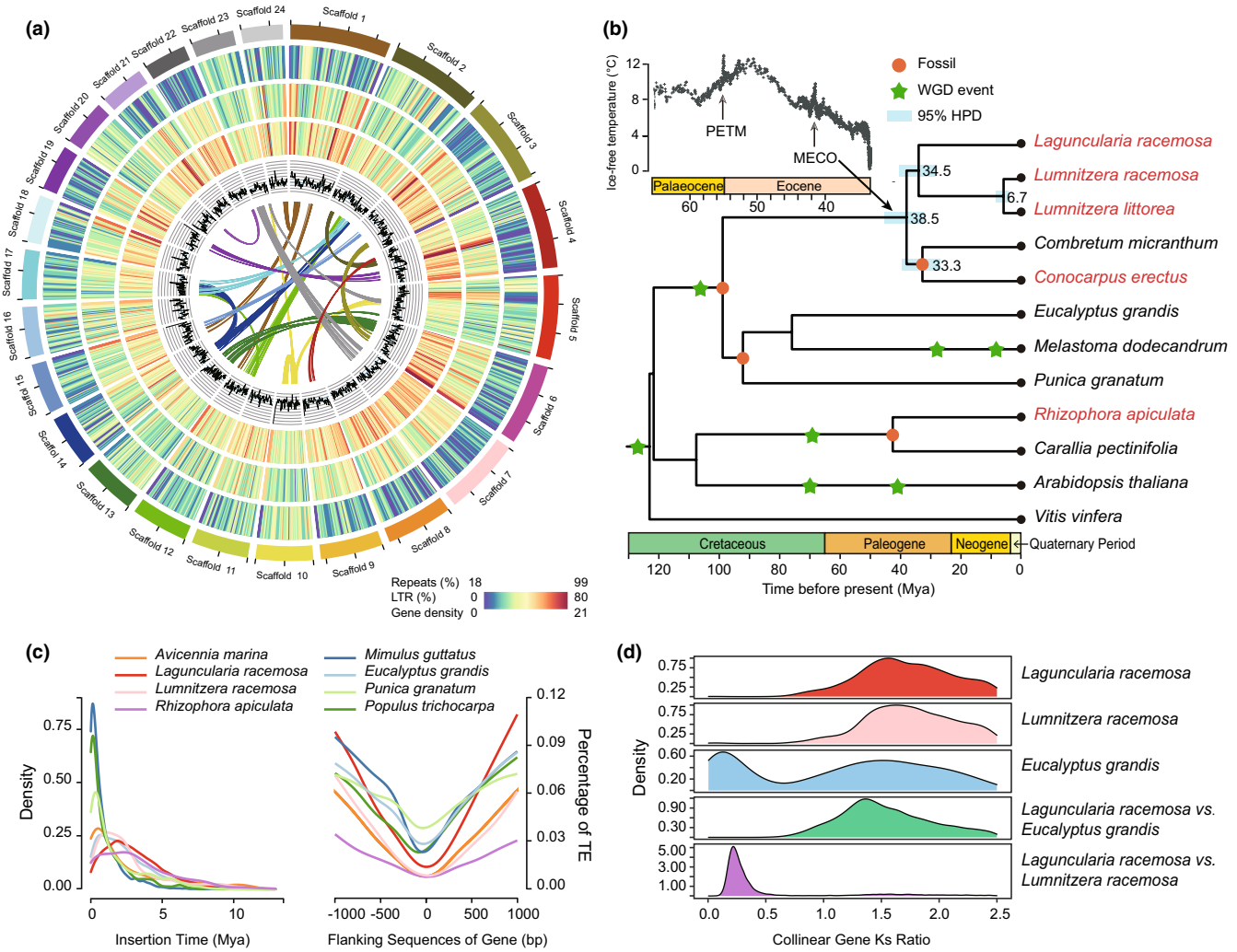

FIGURE 2 Genome features, phylogeny and genome evolution. (a) *Laguncularia racemosa* genome features. Each linking line in the centre of the circle connects a pair of homologous genes. Circular tracks represent, from inner to outer, GC content (31.17%–40.24% per 200 Kb), repeat sequences (17.93%–98.55% per 200 Kb), LTRs (0%–80.12% per 200 Kb), gene number (0–21 per 200 Kb) and scaffold length. The calibration tails are 5 Mb apart. The plot was generated using Circos (http://www.circos.ca/). (b) Phylogenetic tree of *L. racemosa* and its relatives. Estimated divergence times of Combretaceae species are shown beside the nodes. The blue node bars are 95% confidence intervals. Red dots indicate the four fossil calibration nodes (see Section 2). Mangrove species are marked in red. The inset on the top left shows that historical climate change was adapted from Zachos et al. (2008). (c) Low TE activity of *L. racemosa* and other mangroves. The left panel shows LTR element insertion time distributions. The mutation rate is 6.23×10^{-9} per bp per year. The right panel shows TE content in gene flanking regions. Negative numbers on the *x*-axis represent positions upstream and positive numbers downstream of genes. (d) Distribution of synonymous substitutions (Ks) between collinear genes within and between species. The Ks peak within species suggests whole-genome duplication events and the Ks peak between species represents species divergence.

genes annotated as transcription factors, classified into 73 families (Table S5). Among them, MYB, C2H2, AP2, BHLH and NAC are the dominant classes.

3.3 | Intertidal zone invasion during global warming events

Using the whole-genome sequences, we first inferred the *L. racemosa* origin time. Its invasion of intertidal zones from inland ancestors can be constrained since it must have occurred after divergence from inland species and before separation from closely related mangroves. The Combretaceae mangrove genus *Lumnitzera*, considered to be the closest *Laguncularia* relative, the inland plant *C. micranthum* and another mangrove species *C. erectus* were used for the inference. With an additional seven plant genomes, we identified 938 highly conserved single-copy orthologs to reconstruct a phylogenetic tree using RAxML (Stamatakis, 2014). Consistent with previous studies, the closest *L. racemosa* relative is the *Lumnitzera* genus comprising mangrove species *Lumnitzera racemosa* and *Lumnitzera littorea*. *Combretum micranthum* and *Conocarpus erectus* form a sister group (Figure 2b; Figure S4; Tan et al., 2002).

This phylogeny, particularly the fact that the *Laguncularia* and *Lumnitzera* genera include only mangrove species, suggests that the

mangrove genera diverged in a single event from inland ancestors. However, their relationship with the inland plant genus *Macropteranthes*, not included in our analysis because no full genome sequences are available, is in an unclear relationship with the two mangrove genera (Berger et al., 2016). We, thus, expanded our taxonomic sampling and reconstructed a phylogeny containing the three genera already used and eight additional Combretaceae species. The expanded sampling could only be accomplished by considering a small subset of genes. We used *ndhf*, *psaA* and *rbcl* loci (Figure S5). The expanded phylogeny still supports *Laguncularia* and *Lumnitzera* as the most closely related genera, indicating a single mangrove origin.

We then inferred divergence times using a Bayesian approach that takes advantage of four known fossils for calibration, implemented in MCMCTREE (Figure 2b; Yang, 2007). Since *Laguncularia* and *Lumnitzera* share the same ancestor, we treated their divergence as the lower limit on the origin time. Divergence from the *Combretum–Conocarpus* ancestor is then the upper limit. We estimate the lower limit of the *Laguncularia–Lumnitzera* mangrove origin at 34.5 Mya and the upper limit at 38.5 Mya. Just before that period, the Middle Eocene Climate Optimum (MECO, ~40 Mya) resulted in global warming of over 4°C, resulting in drastic sea level elevation (Zachos et al., 2008). The rapid sea level rise caused by global warming may have forced the ancestors to adapt to intertidal environments. The subsequent cooling may have led to the divergence between *Laguncularia* and *Lumnitzera*, whose natural distributions are mutually exclusive.

3.4 | No recent TE activation or WGD events in *L. racemosa* genome

Activation of transposable elements (TEs) introduces many genetic changes and has been proposed to play important roles in rapid environmental adaptation of introduced species (Stapley et al., 2015). 66.96% (740 Mb) of the *L. racemosa* genome consists of repetitive sequences, with long terminal repeat retrotransposons (LTRs) accounting for 44.60% (492 Mb) of the genome (Table S3; Figure S6). This contrasts with previous studies of three independent mangrove clades that found small genomes and few transposable elements in each case (3.14%–8.16% of the genome consisting of TEs; Lyu et al., 2018).

Despite the high TE incidence, we found that TE activity is low in *L. racemosa*. Our estimates of LTR retrotransposon insertion rates are lower in *L. racemosa* and other mangroves than in non-mangroves over the past 5 million years (Figure 2c). Insertion of TEs in or near genes usually represses gene expression by interrupting promoter regions (Lerat & Sémon, 2007). We found fewer transposable elements 500 bp or closer to genes in *L. racemosa* and other mangroves than in non-mangroves (Figure 2c), suggesting little influence on overall gene expression. Furthermore, there are 1942 processed pseudogenes that originate from TE-dependent reverse transcription events in *L. racemosa*, fewer than the 3179 in its relatives (Table S6). This evidence strongly suggests that TE activity is repressed in the *L. racemosa* genome despite high extant transposable element abundance. This is in line with observations from all mangrove genomes available to date (Lyu et al., 2018). TEs do not appear to have played a role in *L. racemosa*'s rapid environmental adaptation after it invaded intertidal zones.

Whole-genome duplications (WGDs) that produce many gene duplications are also major driving forces of rapid environmental adaptation (Feng et al., 2023; Magadum et al., 2013; Van de Peer et al., 2017; Xu et al., 2023). We identified 181 syntenic block pairs (>five homologous gene pairs) in the *L. racemosa* genome, comprising 2981 (14.12%) protein-coding genes. While such syntenic blocks often indicate a past WGD event, the between-homologue Ks (synonymous substitution rate) distribution across syntenic blocks has a peak of around 1.3–1.7, larger than the divergence between *L. racemosa* and *E. grandis* (Figure 2d). Thus, we find no evidence of recent large-scale gene duplications in *L. racemosa*. To confirm the results, we performed a syntenic analysis between *L. racemosa* and *V. vinifera*, which experienced no WGD after the ancient γ event. We estimated that 66% and 45% of genes in the two species show collinearity with the other species. Among them, 1864 *V. vinifera* genes are in two or more syntenic blocks in *L. racemosa*, but only 51 *L. racemosa* genes are in two or more such blocks in *V. vinifera* (Figure S7). These results are consistent with the previously identified lineage-specific WGD event in the ancestor of Myrtales and indicate no recent WGD events in *L. racemosa* (Hao et al., 2022; Myburg et al., 2014).

3.5 | Evolution of gene families and fast growth, intense light and cold tolerance

3.5.1 | Gene family clustering and tandem gene duplication identification

In addition to TEs and WGDs, individual (e.g. tandem) gene duplications result in gene copy number variation that often contributes to environmental adaptation (Hu et al., 2023; Wang et al., 2021). To identify tandem duplications, we first performed gene family clustering in species used for phylogeny reconstruction described above. The 21,070 *L. racemosa* protein-coding genes were clustered into 15,183 gene families, 56 of which significantly expanded and 142 contracted (Table S7).

We identified 1199 tandemly duplicated gene clusters in the *L. racemosa* genome, involving 3166 genes. The proportion of tandem duplications is higher than in mangrove clades that experienced WGDs (*Avicennia*, *Rhizophora*; Table S8). Among mangroves, genomes of species without recent WGD (*C. erectus*, *L. racemosa* and *Lumnitzera racemosa*) have more functional GO terms and KEGG pathways overrepresented among tandemly duplicated genes than genomes that show strong signals of recent whole-genome duplications (*A. marina* and *R. apiculata*; Figures S8–S10). This suggests that tandem gene duplications are an important source of raw material for evolution. We see an overrepresentation of GO terms describing secondary metabolic and defence response processes, suggesting the role of tandem gene duplication in local environment adaptation.

3.5.2 | Tandem gene duplications and mangrove reforestation

One of the overrepresented GO terms is cation transport which plays key roles in a wide range of physiological functions in plants. There are 36 *L. racemosa* gene families that are involved in cation transmembrane transport, contributing to pollen development, metal ion transport and high salt stress tolerance (Figure 3a; Table S9). Specifically, natural resistance-associated macrophage protein (*NRAMP*) and zinc transporter (*ZIP*) families contribute to preventing heavy metal toxicity and maintaining the absorption of trace elements (Gao et al., 2018; Milner et al., 2013). Amino acid permease (*AAP*) and multidrug and toxic compound extrusion (*MATE*) gene families contribute to high salt damage protection (Covarrubias et al., 2017; Pereira et al., 2019). Phosphor-base N-methyltransferases (*PMT*) 1 and 2 are transcriptionally induced by Pi starvation to maintain leaf growth (Ngo et al., 2022). Plasma membrane-localized calcium ATPases (*ACA*) 12 and 13 proteins are induced by UVB and osmotic stress and are involved in inflorescence and vegetative growth (Figure S11; Limonta et al., 2014; Yu et al., 2018). The species-specific tandem duplication of these genes in *L. racemosa* may have promoted fast growth and adaptation to stressful intertidal environments.

One of the most noticeable traits distinguishing *L. racemosa* from other mangrove plants is its fast growth (Berger et al., 2006). Correspondingly, tandem gene duplications in *L. racemosa* are uniquely enriched in GO terms describing auxin biosynthesis processes (Figure 3a,b). Ten gene families are involved in this process and all of them have undergone tandem duplications in *L. racemosa*, while in the close relative *Lumnitzera racemosa*, six of 10 such gene families did not show any tandem duplication (Figure 3b; Table S10). Among those gene families, the cytochrome P450 *CYP79B*, aldehyde oxidase (*AAO*), nitrilases (*NIT*) and acylamidohydrolase (*AMI1*) gene families belong to indole-3-acetic acid (IAA) biosynthesis pathways (Di et al., 2016). Interestingly, *Eucalyptus grandis*, another fast-growing species, also harbours gene duplications disproportionally involved in hormone metabolic processes.

In addition to fast growth, another feature of *L. racemosa* is its tolerance of high light intensity, making it suitable for forest restoration in mudflats as a pioneer species. We examined the plant's "response to high light intensity" pathway and found a conserved gene copy number among species. However, we still found that the ethylene response factor *ERF5/6* gene family involved in high light intensity tolerance experienced species-specific tandem duplications in *L. racemosa* (four in *L. racemosa* and one in *Lumnitzera racemosa*). The *EFR6* gene family protein is a positive antioxidant regulator that can rapidly respond to intense light (Figure 3e,f). It promotes stress defence via transcriptional activation of *WRKY33*, *STZ* and *MYB51* when exposed to osmosis (Dubois et al., 2013; Vogel et al., 2014). Phylogenetic analysis shows that the *ERF5/6* gene family forms two clades in Combretaceae (Figure 3e). Tandem duplication in *L. racemosa* after its divergence from *Lumnitzera racemosa* created three extra *ERF5/6* copies.

Low temperature at high latitudes is a major factor constraining mangrove distribution. However, *L. racemosa* can tolerate low temperatures and grow well when planted in high-latitude intertidal zones (Li et al., 2020; Zhang et al., 2023). Among the genes involved in plant cold tolerance pathways, we found that the C-repeat-binding factor (*CBF*) coding gene has a species-specific tandem duplication from two copies in *Lumnitzera racemosa* to 11 copies in *L. racemosa* (see Section 2; Figure 3c; Figure S12). CBFs bind to promoter sequences and regulate 10%–15% of cold-responsive genes (Gong et al., 2020). Overexpression of *CBF* genes can increase freezing tolerance without a low-temperature stimulus (Wisniewski et al., 2015). All the tandemly duplicated copies retained conserved functional domains, indicating functionality.

All the *L. racemosa CBF* copies show low expression in normal conditions and can be activated by cold treatment, indicating the involvement in cold response of all duplicated copies. Interestingly, some of the copies were activated rapidly within 3 h, while others were activated later or even in the recovery stage (Figure 3d). Such differential response *CBF* may facilitate the survival of *L. racemosa* under cold stress and promote its recovery to normal physiological function upon returning to optimal temperature.

3.6 | Convergent evolution with locally dominant mangroves

When used for reforestation, *L. racemosa* tolerates a wide range of salt levels and is resistant to low nutrition stress found in intertidal zones. To explore potential molecular mechanisms underlying these phenotypes, we chose three dominant native mangroves and tested their genomes for convergent evolution with *L. racemosa*.

3.6.1 | Convergent amino acid substitutions and tolerance to low nutrition

We identified 6266 high-confidence orthologs among *L. racemosa*, three native mangrove species (*A. marina*, *R. apiculata* and *A. corniculatum*) and their inland relatives. Of these, 15 genes carry convergent AA substitutions in all four mangroves, while no such pattern was found in the control non-mangrove group (p-value $= 3.0 \times 10^{-5}$, Fisher's exact test; Figure 4a; Table S11).

Genes harbouring these convergent AA substitutions are homologous to loci involved in nutrient transport and stress tolerance (Table S11). Specifically, copper amine oxidase (*CuAO*) helps cell walls strengthen under wound healing and pathogen attack (Fraudentali et al., 2021). Alpha-amylases 3 (*AMY3*) are chloroplast-localized endo-acting enzymes that can accelerate starch degradation contributing to osmotic balance and protecting the photosynthetic apparatus from oxidative stress (Thalmann et al., 2016).

Two convergently evolving genes are involved in nutrient uptake. The *PHT4;2*, encoding a plastid-localized phosphate transporter, contributes to Pi transport in roots (Fabiańska et al., 2019).

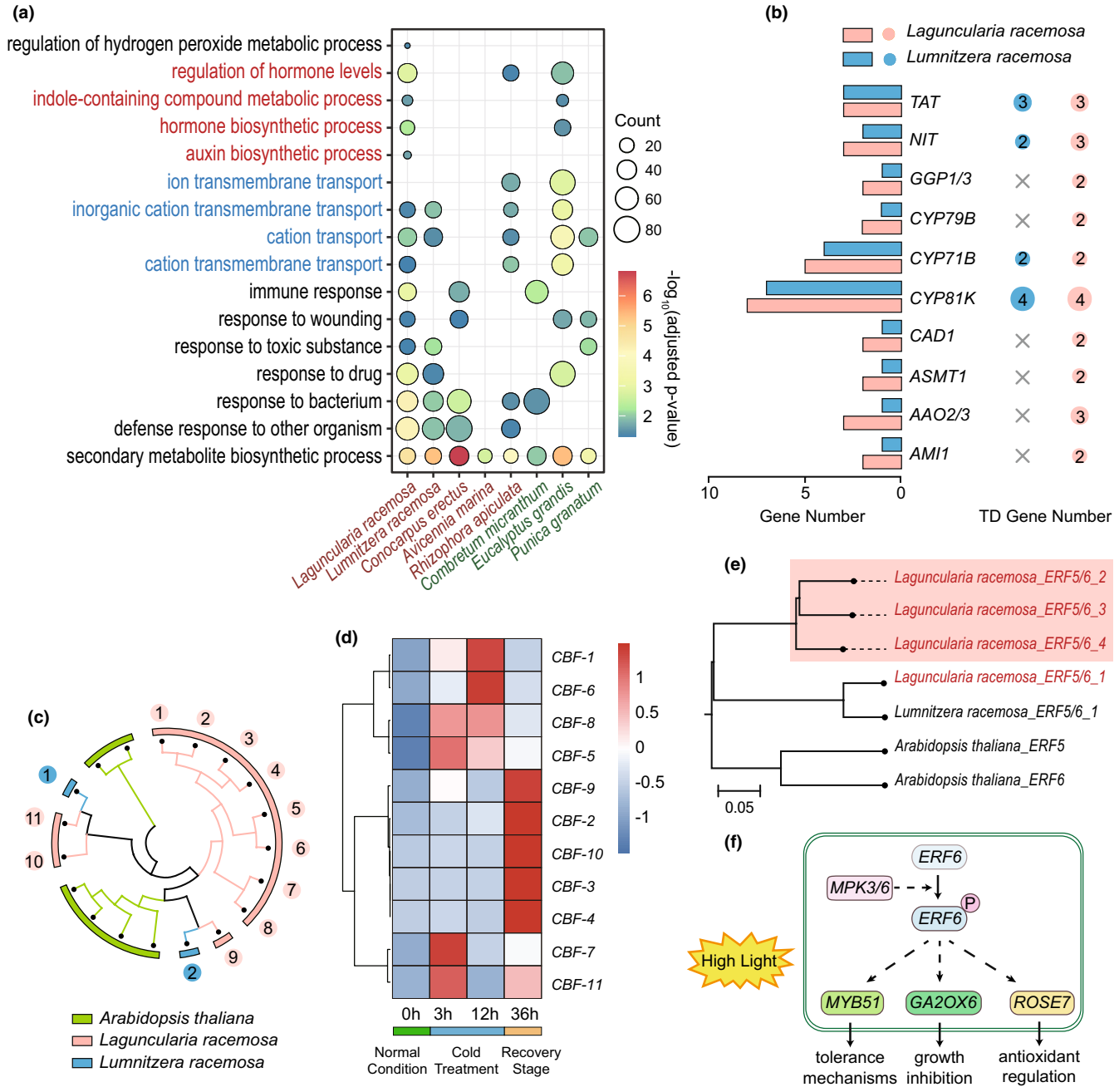

FIGURE 3 Tandem gene duplication and properties related to reforestation. (a) GO terms are overrepresented among tandem duplicated gene families. The size and colour of bubbles represent gene numbers; *p*-values were calculated using Fisher's exact test. The red and blue labels indicate hormone and ion transport-related GO terms. (b) Gene families involved in auxin biosynthesis are overrepresented in *Laguncularia racemosa*. The pink and blue represent *L. racemosa* and *Lumnitzera racemosa* respectively. Bar heights reflect gene family sizes. Dot sizes represent numbers of tandem duplicated genes in each family and crosses-mark families with no tandem duplication. (c) Phylogenetic analysis of the *CBF* gene family in *Arabidopsis thaliana*, *L. racemosa* and *Lumnitzera racemosa*. The green, pink and blue represent *A. thaliana*, *L. racemosa* and *Lumnitzera racemosa* respectively. The numbers represent *CBF* gene copies in *Laguncularia racemosa* and *Lumnitzera racemosa*. (d) Heatmap of the *CBF* gene expression in *L. racemosa* during experimental cold treatment. Each column represents a different treatment stage. Each row represents a gene copy. Gene expression among stages is normalized using *z*-scores. (e) Phylogenetic analysis of the *ERF5/6* gene family in *A. thaliana*, *L. racemosa* and *Lumnitzera racemosa*. The red names represent *L. racemosa*, and black marks the other species. (f) The *ERF6* signalling pathway. Solid and dotted arrows represent direct and indirect interactions respectively.

NRT2.5, encoding a plasma membrane-localized high-affinity nitrate transporter, improves NO_3 transport efficiency (Figure 4b; Ruffel et al., 2021). The A149S convergent substitution in *NRT2.5* exists in only six of more than 200 orthologs from inland plants found in the UniProt database (Figure 4c; Table S12). We further found that the same derived amino acid is shared by all sister species in multi-species mangrove clades *Avicennia* (four species), Rhizophoraceae (nine species) and *Lumnitzera* (two species; sister species

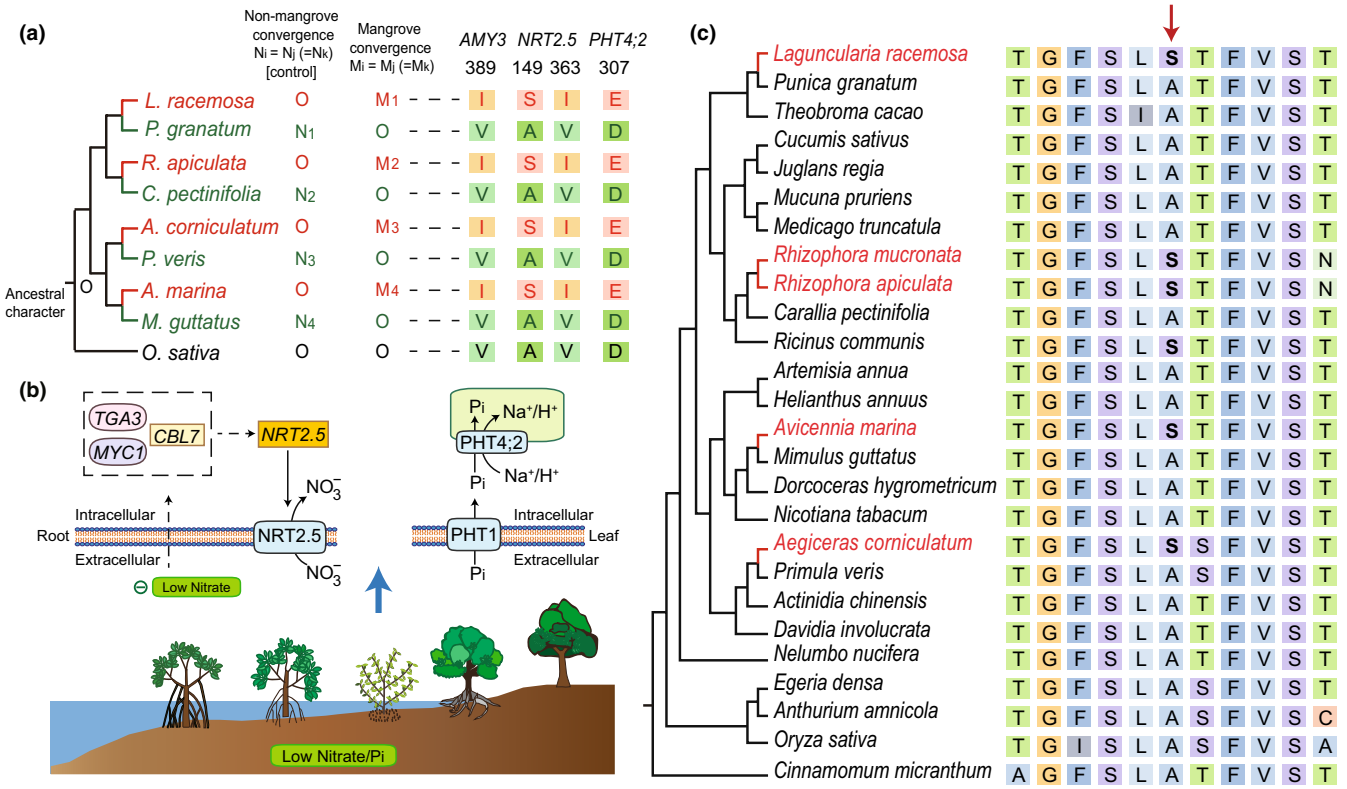

FIGURE 4 Convergent evolution at conservative sites in *Laguncularia racemosa* and three dominant native mangroves. (a) Convergent site inference. The cladogram consists of four mangrove:non-mangrove pairs as ingroup species and *O. sativa* as the outgroup. O indicates the outgroup state, M_i is the character in mangroves and N_i is the non-mangrove state. Mangrove convergence is inferred at conservative sites where all non-mangroves retain the same character as the outgroup, i.e., $N_1 = N_2 = N_3 = O$. Among the conservative sites, mangrove convergence is assigned if $M_1 = M_2 = M_3 \neq O$. The right panel shows examples of convergently evolving mangrove genes. Positions are aligned to *O. sativa* protein sequences. (b) Sketch map of the signalling pathways with convergently evolving genes *NRT2.5* and *PHT4;2*. (c) A convergent amino-acid change A149S in *NRT2.5* shared by independent mangroves at the alignment position indicated by the red arrow. The tree was constructed using APG IV system with red branches and names representing mangroves.

of *L. racemosa*), but not in the most closely related inland species (Figure S13). It, thus, appears that the A149S substitution in *NRT2.5* has occurred after divergence from inland relatives and before differentiation among sister species. The derived amino acid sequence in *L. racemosa* may improve its adaptability to nitrate starvation in intertidal zones (Reef et al., 2010).

3.6.2 | Convergent gene copy number variation and salt tolerance

To focus on high salt tolerance, we examined convergently derived copy number changes between *L. racemosa* and the three native mangrove species. Among 515 gene families involved in high salinity tolerance, we identified more convergent changes in mangroves than in control inland species (Figure 5a,b). Specifically, there is one convergent expansion and six convergent contractions of gene families in four non-mangroves, while there are three and 11 in mangroves (Figure 5b, Table S13).

Gene families that experienced convergent expansions in mangroves include *GST30*, *SAP5* and *ATGRP7*. For example, *SAP5* has two to eight copies in mangrove species (3.75 on average), but only two to four in non-mangroves (1.75 on average). The gene exhibits E3 ubiquitin ligase activity and may be induced by salt stress. It improves salt tolerance by up-regulating the expression of endogenous stress-responsive genes such as *AtGols2* and reducing average stomatal apertures, acting as a positive regulator of the stress response (Kang et al., 2011).

The most significant convergent gene contraction occurred in the *RAS1* (Response to ABA and Salt 1) family, a negative regulator of salt tolerance (Ren et al., 2010). Gene family clustering shows that the *RAS1* was completely lost in *L. racemosa* and native mangroves *A. marina* and *R. apiculata*, and was fragmented in *A. corniculatum* (Figure 5d). This conclusion is further supported by homologous sequence search throughout genome assemblies, and the microsynteny of *RAS1* and its 10 neighbouring genes among mangrove:non-mangrove pairs (Section 2; Figure 5d). This indicates that the *RAS1* gene is convergently lost in *L. racemosa* and the three native mangrove species.

The abscisic acid (ABA) biosynthesis pathway is induced by exposure to salt stress, initiating downstream gene expression via ABA signalling, and inhibiting seed germination. *RAS1* is a positive

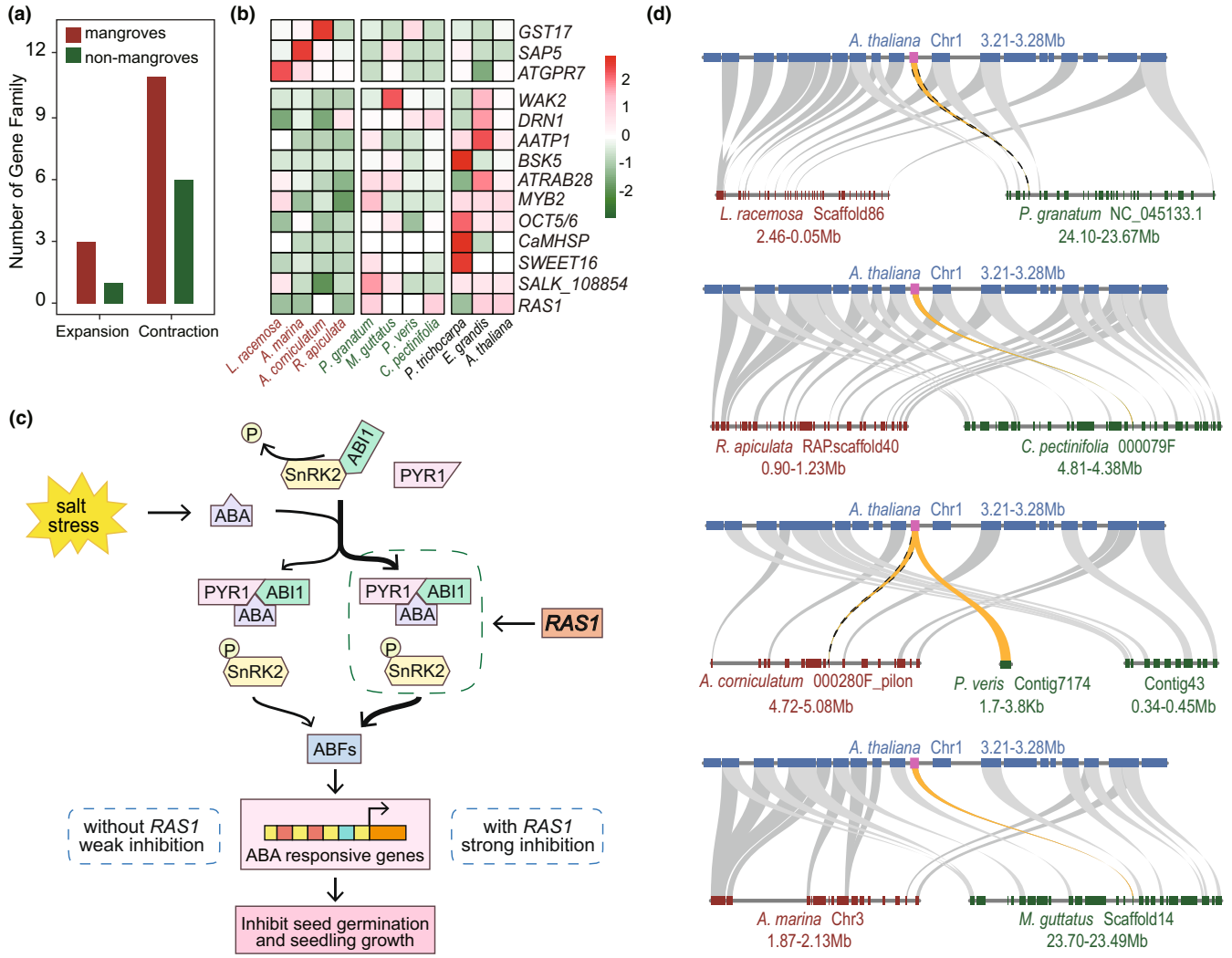

FIGURE 5 Convergent gene copy number variation in *Laguncularia racemosa* and three dominant native mangroves. (a) More convergent gene copy number changes in mangroves than in non-mangroves. (b) Convergently expanded or contracted mangrove gene families. In each gene family, gene numbers among species are normalized using *z*-scores. (c) The hypothesized *RAS1* signalling pathway. The dotted box represents the interaction between ABA and its receptor. (d) Collinearity of *RAS1* and its neighbouring genes between *Arabidopsis thaliana* and four mangrove: non-mangrove pairs. Diamonds represent genic regions and the *RAS1* gene is highlighted in purple. The dotted lines indicate fragmentary gene copies.

regulator of core ABA signalling, regulating the interaction between abscisic acid insensitive 1 (*ABI1*) and ABA receptor pyrabactin resistance 1 (*PYR1*) (Figure 5c; Nakashima & Yamaguchi-Shinozaki, 2013; Ren et al., 2010). Since the loss of *RAS1* has been shown to decrease ABA sensitivity and enhance salt tolerance in *A. thaliana*, the convergent loss of *RAS1* should result in high salt tolerance of *L. racemosa* and the other mangroves.

4 | DISCUSSION

Ecological restoration of the mangrove ecosystem is receiving increasing attention because this ecosystem is crucial but has experienced a heavy global decline. Non-native species are often used for restoration because of their fast growth and high adaptability, which may also make them invasive species. In this study, we assembled a high-quality reference genome of *L. racemosa*, a dominant mangrove species in AEP that is used for ecological restoration of mangrove forests in China (He et al., 2022; Tomlinson, 2016; Xie et al., 2022; Zhong et al., 2011). We inferred the origin of this newly sequenced mangrove clade in line with a global warming event. By performing comparative genomic analyses, we explored why *L. racemosa* adapts as well to stressful intertidal environments as natively dominant mangroves and why it grows quickly and tolerates intense light and low temperatures. Our results point to genomic features that underpin the advantages of the non-native *L. racemosa* as a mangrove reforestation species, and also provide molecular insight for its potential invasiveness evaluation.

Like previously reported mangrove clades, *L. racemosa* originated during a global warming event (He et al., 2020; Xu et al., 2017). After invading intertidal zones, this mangrove clade diverged into *Laguncularia* and *Lumnitzera*, currently occupying Atlantic-East Pacific (AEP)

and Indo-West Pacific (IWP) regions respectively (Figure S1; Tomlinson, 2016; Xie et al., 2022). Given the weak dispersal ability of their seeds and the long distances across the Pacific Ocean, we speculate that the ancestor invaded intertidal zones in North Africa and dispersed in two main directions with the African continent as the boundary (Fuster-Calvo et al., 2021). Subsequent tectonic plate movements blocked gene flow resulting in species divergence (Potter & Szatmari, 2009).

As a pioneer mangrove species used for reforestation, *L. racemosa* differs from other mangroves. It grows quickly and tolerates intense light and cold. These properties may be caused by species-specific genetic changes such as activation of TEs, WGDs or tandem gene duplications. However, the *L. racemosa* genome does not have many active TEs and does not appear to have undergone recent WGDs that often promote rapid environmental adaptation. Although the *L. racemosa* genome is rich in transposable elements, their activity is repressed and may contribute little to rapid environmental adaptation. Instead, TE activity repression seems to be a common strategy among mangrove species to maintain genome stability in fluctuating intertidal zones (Lyu et al., 2018).

Despite no WGDs or activated TEs, *L. racemosa* genome is rich in tandem gene duplications. Compared with its closely related mangrove *Lumnitzera racemosa*, species-specific tandem duplications have occurred in many genes involved in auxin biosynthesis. Key transcription factors that activate downstream responsive genes involved in intense light and cold tolerance also experienced tandem duplications (e.g. *ERF6* and *CBFs*). These tandem gene duplications may explain *L. racemosa*'s fast growth when introduced into mudflats or grown at high latitudes. This is consistent with previous reports that tandem gene duplications tend to be involved in rapid environmental adaptation (Myburg et al., 2014; Wang et al., 2021).

Successful reforestation of intertidal zones also requires adaptation to environmental stressors such as extremely high salinity and low nutrition. We identified convergently evolved amino acid site substitutions and copy number variations among *L. racemosa* and three dominant native mangroves. In particular, the convergent AA substitution A149S in the *NRT2.5* gene encoding a nitrogen transporter likely occurred during the invasion of intertidal zones (Ruffel et al., 2021). The extensive convergent expansion/reduction of genes involved in salt stress resistance, such as the loss of the *RAS1* gene, are strong signals of adaptive evolution. The convergent changes may be important for the wide distribution of native mangroves and the reforestation in exposed mudflats using *L. racemosa*.

Our results also indicate that *L. racemosa* could become invasive (Gu et al., 2019; Li et al., 2020). Field surveys suggest that *L. racemosa* grows quickly and has the potential to outcompete native mangrove species. The obtained genomic changes render *L. racemosa* resistant to high salinity and low nutrition to an extent comparable to the widely distributed IWP mangroves. In addition, tandem gene duplications allow *L. racemosa* to produce more seedlings and tolerate more intense light and cold than other mangroves. These may confer on *L. racemosa* the potential to replace native mangrove species or even decrease species diversity of native ecological communities. Indeed, many ecological and physiological field surveys indicate that *L. racemosa* grows better than native mangroves and shows potential invasiveness like *Sonneratia apetala* (Feng et al., 2021; Li et al., 2020). In addition, *L. racemosa's* genetic diversity is higher than most IWP region mangroves (He et al., 2022). This increased heterozygosity may allow *L. racemosa* to survive in various environments where it is introduced (Guo et al., 2018). Overall, our comparative genomic analyses identified mechanisms of *L. racemosa* intertidal adaptation that is shared with dominant native mangrove species. The identification of the molecular mechanisms underlying fast growth, intense light and cold tolerance also provides the basis for evaluating *L. racemosa*'s invasiveness potential and informing decisions about its use for ecological restoration.

ACKNOWLEDGEMENTS

We thank Professor Chung-I Wu at Sun Yat-sen University for his suggestions on the manuscript. We thank Dr. Yuchen Yang at Sun Yat-sen University for providing transcriptome data. This study was supported by the National Natural Science Foundation of China (31830005 and 32100176); the Guangdong Basic and Applied Basic Research Foundation (2020A1515110164 and 2022A1515010962) and the Innovation Group Project of Southern Marine Science and Engineering Guangdong Laboratory (Zhuhai) (No. 311021006).

CONFLICT OF INTEREST STATEMENT

The authors declare that they have no competing interests.

DATA AVAILABILITY STATEMENT

The genome sequence was deposited at GenBank of BioProject PRJNA905396 and National Genomics Data Center (NGDC, https://ngdc.cncb.ac.cn/) under accession no. GWHBEBM00000000.

ORCID

Suhua Shi https://orcid.org/0000-0003-2809-5999
Shaohua Xu https://orcid.org/0000-0002-4379-2621

REFERENCES

Anders, S., & Huber, W. (2010). Differential expression analysis for sequence count data. *Genome Biology*, *11*, R106.

Berger, B. A., Kriebel, R., Spalink, D., & Sytsma, K. J. (2016). Divergence times, historical biogeography, and shifts in speciation rates of Myrtales. *Molecular Phylogenetics and Evolution*, *95*, 116–136.

Berger, U., Adams, M., Grimm, V., & Hildenbrandt, H. (2006). Modelling secondary succession of neotropical mangroves: Causes and consequences of growth reduction in pioneer species. *Perspectives in Plant Ecology, Evolution and Systematics*, *7*(4), 243–252.

Besemer, J., Lomsadze, A., & Borodovsky, M. (2001). GeneMarkS: A self-training method for prediction of gene starts in microbial genomes. Implications for finding sequence motifs in regulatory regions. *Nucleic Acids Research*, *29*(12), 2607–2618.

Cantalapiedra, C. P., Hernández-Plaza, A., Letunic, I., Bork, P., & Huerta-Cepas, J. (2021). eggNOG-mapper v2: Functional annotation, orthology assignments, and domain prediction at the metagenomic scale. *Molecular Biology and Evolution*, *38*(12), 5825–5829.

Castresana, J. (2000). Selection of conserved blocks from multiple alignments for their use in phylogenetic analysis. *Molecular Biology and Evolution*, *17*(4), 540–552.

Chen, Y., Chen, Y., Shi, C., Huang, Z., Zhang, Y., Li, S., Li, Y., Ye, J., Yu, C., Li, Z., Zhang, X., Wang, J., Yang, H., Fang, L., & Chen, Q. (2018). SOAPnuke: A MapReduce acceleration-supported software for integrated quality control and preprocessing of high-throughput sequencing data. *GigaScience*, *7*(1), gix120.

Chin, C.-S., Peluso, P., Sedlazeck, F. J., Nattestad, M., Concepcion, G. T., Clum, A., Dunn, C., O'Malley, R., Figueroa-Balderas, R., Morales-Cruz, A., Cramer, G. R., Delledonne, M., Luo, C., Ecker, J. R., Cantu, D., Rank, D. R., & Schatz, M. C. (2016). Phased diploid genome assembly with single-molecule real-time sequencing. *Nature Methods*, *13*(12), 1050–1054.

Covarrubias, A. A., Sharma, S., Borsani, O., Chen, Y., Zhang, M., Chen, J., Wang, T., Liu, J., Han, H., & Hua, X. (2017). Arabidopsis AMINO ACID PERMEASE1 contributes to salt stress-induced proline uptake from exogenous sources. *Frontiers in Plant Science*, *8*, 2182.

Di, D.-W., Zhang, C., Luo, P., An, C.-W., & Guo, G.-Q. (2016). The biosynthesis of auxin: How many paths truly lead to IAA? *Plant Growth Regulation*, *78*(3), 275–285.

Doyle, J. J., & Doyle, J. L. (1987). A rapid DNA isolation procedure for small quantities of fresh leaf tissue. *Phytochemical Bulletin*, *19*, 11–15.

Dubois, M., Skirycz, A., Claeys, H., Maleux, K., Dhondt, S., De Bodt, S., Vanden Bossche, R., De Milde, L., Yoshizumi, T., Matsui, M., & Inzé, D. (2013). Ethylene response factor6 acts as a central regulator of leaf growth under water-limiting conditions in Arabidopsis. *Plant Physiology*, *162*(1), 319–332.

Dudchenko, O., Batra, S. S., Omer, A. D., Nyquist, S. K., Hoeger, M., Durand, N. C., Shamim, M. S., Machol, I., Lander, E. S., Aiden, A. P., & Aiden, E. L. (2017). De novo assembly of the *Aedes aegypti* genome using Hi-C yields chromosome-length scaffolds. *Science*, *356*(6333), 92–95.

Durand, N. C., Shamim, M. S., Machol, I., Rao, S. S., Huntley, M. H., Lander, E. S., & Aiden, E. L. (2016). Juicer provides a one-click system for analyzing loop-resolution Hi-C experiments. *Cell Systems*, *3*(1), 95–98.

Edgar, R. C. (2004). MUSCLE: A multiple sequence alignment method with reduced time and space complexity. *BMC Bioinformatics*, *5*(1), 113.

Emms, D. M., & Kelly, S. (2019). OrthoFinder: Phylogenetic orthology inference for comparative genomics. *Genome Biology*, *20*(1), 238.

Fabiańska, I., Bucher, M., & Häusler, R. E. (2019). Intracellular phosphate homeostasis – A short way from metabolism to signaling. *Plant Science*, *286*, 57–67.

Fang, F., Li, Z., & Gui, H. (2022). Investigation and research on current situation of mangrove in Hainan. *Tropical Forestry*, *50*(1), 42–49.

Feng, H., Gu, X., Tang, T., Lin, Q., Ratul, S. B., Wang, X., & Chen, L. (2021). Determining the effects of salinity and light on key ecophysiological traits of two nonnative mangrove species in China. *Journal of Coastal Research*, *38*(2), 361–368.

Feng, X., Li, G., Wu, W., Lyu, H., Wang, J., Liu, C., Zhong, C., Shi, S., & He, Z. (2023). Expansion and adaptive evolution of the WRKY transcription factor family in Avicennia mangrove trees. *Marine Life Science & Technology*, *5*(2), 155–168.

Fraudentali, I., Rodrigues-Pousada, R. A., Angelini, R., Ghuge, S. A., Cona, A., & Phan Tran, L.-S. (2021). Plant copper amine oxidases: Key players in hormone signaling leading to stress-induced phenotypic plasticity. *International Journal of Molecular Sciences*, *22*(10), 5136.

Fuster-Calvo, A., Nogales, M., Heleno, R., Vera, C., & Vargas, P. (2021). Sea dispersal potential and colonization of the Galápagos littoral flora. *Journal of Biogeography*, *48*(8), 1904–1916.

Gao, H., Xie, W., Yang, C., Xu, J., Li, J., Wang, H., Chen, X., & Huang, C.-F. (2018). NRAMP2, a trans-Golgi network-localized manganese transporter, is required for Arabidopsis root growth under manganese deficiency. *New Phytologist*, *217*(1), 179–193.

Giri, C., Ochieng, E., Tieszen, L. L., Zhu, Z., Singh, A., Loveland, T., Masek, J., & Duke, N. (2011). Status and distribution of mangrove forests of the world using earth observation satellite data. *Global Ecology and Biogeography*, *20*(1), 154–159.

Goldberg, L., Lagomasino, D., Thomas, N., & Fatoyinbo, T. (2020). Global declines in human-driven mangrove loss. *Global Change Biology*, *26*(10), 5844–5855.

Gong, Z., Xiong, L., Shi, H., Yang, S., Herrera-Estrella, L. R., Xu, G., Chao, D.-Y., Li, J., Wang, P.-Y., Qin, F., Li, J., Ding, Y., Shi, Y., Wang, Y., Yang, Y., Guo, Y., & Zhu, J.-K. (2020). Plant abiotic stress response and nutrient use efficiency. *Science China Life Sciences*, *63*(5), 635–674.

Graham, A. (2006). Paleobotanical evidence and molecular data in reconstructing the historical phytogeography of Rhizophoraceae. *Annals of the Missouri Botanical Garden*, *93*(2), 325–334.

Greig-Smith, P. (1983). *Quantitative plant ecology* (Vol. *9*). University of California Press.

Gremme, G., Steinbiss, S., & Kurtz, S. (2013). Genome tools: A comprehensive software library for efficient processing of structured genome annotations. *IEEE/ACM Transactions on Computational Biology and Bioinformatics*, *10*(3), 645–656.

Grímsson, F., Zetter, R., & Hofmann, C.-C. (2011). Lythrum and Peplis from the late cretaceous and Cenozoic of North America and Eurasia: New evidence suggesting early diversification within the Lythraceae. *American Journal of Botany*, *98*(11), 1801–1815.

Gu, X., Feng, H., Tang, T., Tam, N. F.-Y., Pan, H., Zhu, Q., Dong, Y., Fazlioglu, F., & Chen, L. (2019). Predicting the invasive potential of a non-native mangrove reforested plant (*Laguncularia racemosa*) in China. *Ecological Engineering*, *139*, 105591.

Guo, Z., Li, X., He, Z., Yang, Y., Wang, W., Zhong, C., Greenberg, A. J., Wu, C.-I., Duke, N. C., & Shi, S. (2018). Extremely low genetic diversity across mangrove taxa reflects past sea level changes and hints at poor future responses. *Global Change Biology*, *24*(4), 1741–1748.

Haas, B. J., Salzberg, S. L., Zhu, W., Pertea, M., Allen, J. E., Orvis, J., White, O., Buell, C. R., & Wortman, J. R. (2008). Automated eukaryotic gene structure annotation using EVidenceModeler and the program to assemble spliced alignments. *Genome Biology*, *9*(1), R7.

Hao, Y., Zhou, Y. Z., Chen, B., Chen, G. Z., Wen, Z. Y., Zhang, D., Sun, W. H., Liu, D. K., Huang, J., Chen, J. L., Zhou, X. Q., Fan, W. L., Zhang, W. C., Luo, L., Han, W. C., Zheng, Y., Li, L., Lu, P. C., Xing, Y., … Peng, D. H. (2022). The *Melastoma dodecandrum* genome and the evolution of Myrtales. *Journal of Genetics and Genomics*, *49*(2), 120–131.

He, Z., Feng, X., Chen, Q., Li, L., Li, S., Han, K., Guo, Z., Wang, J., Liu, M., Shi, C., Xu, S., Shao, S., Liu, X., Mao, X., Xie, W., Wang, X., Zhang, R., Li, G., Wu, W., … Shi, S. (2022). Evolution of coastal forests based on a full set of mangrove genomes. *Nature Ecology & Evolution*, *6*(6), 738–749.

He, Z., Xu, S., Zhang, Z., Guo, W., Lyu, H., Zhong, C., Boufford, D. E., Duke, N. C., & Shi, S. (2020). Convergent adaptation of the genomes of woody plants at the land–sea interface. *National Science Review*, *7*(6), 978–993.

Hu, X., Jiang, Z., Ming, Y., Jian, J., Jiang, S., Zhang, D., Zhang, J., Zheng, S., Fang, X., Yang, Y., & Zheng, R. (2022). A chromosomal level genome sequence for *Quasipaa spinosa* (Dicroglossidae) reveals chromosomal evolution and population diversity. *Molecular Ecology Resources*, *22*(4), 1545–1558.

Hu, Y., Wang, X., Xu, Y., Yang, H., Tong, Z., Tian, R., Xu, S., Yu, L., Guo, Y., Shi, P., Huang, S., Yang, G., Shi, S., & Wei, F. (2023). Molecular mechanisms of adaptive evolution in wild animals and plants. *Science China Life Sciences*, *66*(3), 453–495.

Huerta-Cepas, J., Szklarczyk, D., Heller, D., Hernández-Plaza, A., Forslund, S. K., Cook, H., Mende, D. R., Letunic, I., Rattei, T., Jensen, L. J., von Mering, C., & Bork, P. (2019). eggNOG 5.0: A hierarchical, functionally and phylogenetically annotated orthology resource based on 5090 organisms and 2502 viruses. *Nucleic Acids Research*, *47*(D1), D309–D314.

Kang, M., Fokar, M., Abdelmageed, H., & Allen, R. D. (2011). Arabidopsis SAP5 functions as a positive regulator of stress responses and exhibits E3 ubiquitin ligase activity. *Plant Molecular Biology*, *75*(4), 451–466.

Kao, W.-Y., Shih, C.-N., & Tsai, T.-T. (2004). Sensitivity to chilling temperatures and distribution differ in the mangrove species *Kandelia candel* and *Avicennia marina*. *Tree Physiology*, *24*(7), 859–864.

Katoh, K., Misawa, K., Kuma, K., & Miyata, T. (2002). MAFFT: A novel method for rapid multiple sequence alignment based on fast Fourier transform. *Nucleic Acids Research*, *30*(14), 3059–3066.

Kim, D., Paggi, J. M., Park, C., Bennett, C., & Salzberg, S. L. (2019). Graph-based genome alignment and genotyping with HISAT2 and HISAT-genotype. *Nature Biotechnology*, *37*(8), 907–915.

Lang, T., Tang, Y., Tam, N. F., Gan, K., Wu, J., Wu, W., Fu, Y., Li, M., Hu, Z., Li, F., Jiang, M., & Zhou, H. (2022). Microcosm study on cold adaptation and recovery of an exotic mangrove plant, *Laguncularia racemosa* in China. *Marine Environmental Research*, *176*, 105611.

Lerat, E., & Sémon, M. (2007). Influence of the transposable element neighborhood on human gene expression in normal and tumor tissues. *Gene*, *396*(2), 303–311.

Li, F. L., Zhong, L., Cheung, S. G., Wong, Y. S., Shin, P. K. S., Lei, A. P., Zhou, H. C., Song, X., & Tam, N. F. Y. (2020). Is *Laguncularia racemosa* more invasive than *Sonneratia apetala* in northern Fujian, China in terms of leaf energetic cost? *Marine Pollution Bulletin*, *152*, 110897.

Li, H., & Durbin, R. (2009). Fast and accurate short read alignment with burrows–wheeler transform. *Bioinformatics*, *25*(14), 1754–1760.

Limonta, M., Romanowsky, S., Olivari, C., Bonza, M. C., Luoni, L., Rosenberg, A., Harper, J. F., & De Michelis, M. I. (2014). ACA12 is a deregulated isoform of plasma membrane Ca2+-ATPase of *Arabidopsis thaliana*. *Plant Molecular Biology*, *84*(4), 387–397.

Luo, X., Li, H., Wu, Z., Yao, W., Zhao, P., Cao, D., Yu, H., Li, K., Poudel, K., Zhao, D., Zhang, F., Xia, X., Chen, L., Wang, Q., Jing, D., & Cao, S. (2020). The pomegranate (*Punica granatum* L.) draft genome dissects genetic divergence between soft- and hard-seeded cultivars. *Plant Biotechnology Journal*, *18*(4), 955–968.

Lyu, H., He, Z., Wu, C. I., & Shi, S. (2018). Convergent adaptive evolution in marginal environments: Unloading transposable elements as a common strategy among mangrove genomes. *New Phytologist*, *217*(1), 428–438.

Magadum, S., Banerjee, U., Murugan, P., Gangapur, D., & Ravikesavan, R. (2013). Gene duplication as a major force in evolution. *Journal of Genetics*, *92*(1), 155–161.

Manchester, S. R., & O'Leary, E. L. (2010). Phylogenetic distribution and identification of fin-winged fruits. *The Botanical Review*, *76*(1), 1–82.

Manni, M., Berkeley, M. R., Seppey, M., Simão, F. A., & Zdobnov, E. M. (2021). BUSCO update: Novel and streamlined workflows along with broader and deeper phylogenetic coverage for scoring of eukaryotic, prokaryotic, and viral genomes. *Molecular Biology and Evolution*, *38*(10), 4647–4654.

Mendes, F. K., Vanderpool, D., Fulton, B., & Hahn, M. W. (2020). CAFE 5 models variation in evolutionary rates among gene families. *Bioinformatics*, *36*(22–23), 5516–5518.

Menéndez, P., Losada, I. J., Torres-Ortega, S., Narayan, S., & Beck, M. W. (2020). The global flood protection benefits of mangroves. *Scientific Reports*, *10*(1), 4404.

Milner, M. J., Seamon, J., Craft, E., & Kochian, L. V. (2013). Transport properties of members of the ZIP family in plants and their role in Zn and Mn homeostasis. *Journal of Experimental Botany*, *64*(1), 369–381.

Muszewska, A., Steczkiewicz, K., Stepniewska-Dziubinska, M., & Ginalski, K. (2019). Transposable elements contribute to fungal genes and impact fungal lifestyle. *Scientific Reports*, *9*(1), 4307.

Myburg, A. A., Grattapaglia, D., Tuskan, G. A., Hellsten, U., Hayes, R. D., Grimwood, J., Jenkins, J., Lindquist, E., Tice, H., Bauer, D., Goodstein, D. M., Dubchak, I., Poliakov, A., Mizrachi, E., Kullan, A. R. K., Hussey, S. G., Pinard, D., van der Merwe, K., Singh, P., … Schmutz, J. (2014). The genome of *Eucalyptus grandis*. *Nature*, *510*(7505), 356–362.

Nakashima, K., & Yamaguchi-Shinozaki, K. (2013). ABA signaling in stress-response and seed development. *Plant Cell Reports*, *32*(7), 959–970.

Ngo, A. H., Angkawijaya, A. E., Lin, Y.-C., Liu, Y., & Nakamura, Y. (2022). The phospho-base *N*-methyltransferases PMT1 and PMT2 produce phosphocholine for leaf growth in phosphorus-starved Arabidopsis. *Journal of Experimental Botany*, *73*(9), 2985–2994.

Ou, S., & Jiang, N. (2018). LTR_retriever: A highly accurate and sensitive program for identification of long terminal repeat retrotransposons. *Plant Physiology*, *176*(2), 1410–1422.

Paul, M., Catterall, C. P., Pollard, P. C., & Kanowski, J. (2010). Does soil variation between rainforest, pasture and different reforestation pathways affect the early growth of rainforest pioneer species? *Forest Ecology and Management*, *260*(3), 370–377.

Pereira, A., Nakashima, K., Zhang, H., Wang, K., Lu, P., Odongo Magwanga, R., Nyangasi Kirungu, J., Hu, Y., Dong, Q., Cai, X., Zhou, Z., Wang, X., Zhang, Z., Hou, Y., & Liu, F. (2019). Overexpression of cotton a DTX/MATE gene enhances drought, salt, and cold stress tolerance in transgenic Arabidopsis. *Frontiers in Plant Science*, *10*, 299.

Potter, P. E., & Szatmari, P. (2009). Global Miocene tectonics and the modern world. *Earth-Science Reviews*, *96*(4), 279–295.

Reef, R., Feller, I. C., & Lovelock, C. E. (2010). Nutrition of mangroves. *Tree Physiology*, *30*(9), 1148–1160.

Ren, Z., Zheng, Z., Chinnusamy, V., Zhu, J., Cui, X., Iida, K., & Zhu, J.-K. (2010). RAS1, a quantitative trait locus for salt tolerance and ABA sensitivity in Arabidopsis. *Proceedings of the National Academy of Sciences*, *107*(12), 5669–5674.

Robinson, J. T., Turner, D., Durand, N. C., Thorvaldsdóttir, H., Mesirov, J. P., & Aiden, E. L. (2018). Juicebox.js provides a cloud-based visualization system for Hi-C data. *Cell Systems*, *6*(2), 256–258.e1.

Rodríguez- Rodríguez, J. A., Mancera Pineda, J. E., Melgarejo, L. M., & Medina Calderón, J. H. (2018). Functional traits of leaves and forest structure of neotropical mangroves under different salinity and nitrogen regimes. *Flora*, *239*, 52–61.

Ruffel, S., Chaput, V., Przybyla-Toscano, J., Fayos, I., Ibarra, C., Moyano, T., Fizames, C., Tillard, P., O'Brien, J. A., Gutiérrez, R. A., Gojon, A., & Lejay, L. (2021). Genome-wide analysis in response to nitrogen and carbon identifies regulators for root AtNRT2 transporters. *Plant Physiology*, *186*(1), 696–714.

Servant, N., Varoquaux, N., Lajoie, B. R., Viara, E., Chen, C.-J., Vert, J.-P., Heard, E., Dekker, J., & Barillot, E. (2015). HiC-Pro: An optimized and flexible pipeline for hi-C data processing. *Genome Biology*, *16*(1), 1–11.

Singh, H., Prasad, M., Kumar, K., Rana, R. S., & Singh, S. K. (2010). Fossil fruits from Early Eocene Vastan Lignite, Gujarat, India: Taphonomic and phytogeographic implications. *Current Science*, *98*(12), 1625–1632.

Slater, G. S. C., & Birney, E. (2005). Automated generation of heuristics for biological sequence comparison. *BMC Bioinformatics*, *6*(1), 31.

Stamatakis, A. (2014). RAxML version 8: A tool for phylogenetic analysis and post-analysis of large phylogenies. *Bioinformatics*, *30*(9), 1312–1313.

Stanke, M., Keller, O., Gunduz, I., Hayes, A., Waack, S., & Morgenstern, B. (2006). AUGUSTUS: Ab initio prediction of alternative transcripts. *Nucleic Acids Research*, *34*(suppl_2), W435–W439.

Stapley, J., Santure, A. W., & Dennis, S. R. (2015). Transposable elements as agents of rapid adaptation may explain the genetic paradox of invasive species. *Molecular Ecology*, *24*(9), 2241–2252.

Suyama, M., Torrents, D., & Bork, P. (2006). PAL2NAL: Robust conversion of protein sequence alignments into the corresponding codon alignments. *Nucleic Acids Research*, *34*(suppl_2), W609–W612.

Tan, F., Shi, S., Zhong, Y., Gong, X., & Wang, Y. (2002). Phylogenetic relationships of Combretoideae (Combretaceae) inferred from plastid,

nuclear gene and spacer sequences. *Journal of Plant Research*, *115*(6), 475–481.

Tang, H., Bowers, J. E., Wang, X., Ming, R., Alam, M., & Paterson, A. H. (2008). Synteny and collinearity in plant genomes. *Science*, *320*(5875), 486–488.

Thalmann, M., Pazmino, D., Seung, D., Horrer, D., Nigro, A., Meier, T., Kölling, K., Pfeifhofer, H. W., Zeeman, S. C., & Santelia, D. (2016). Regulation of leaf starch degradation by abscisic acid is important for osmotic stress tolerance in plants. *The Plant Cell*, *28*(8), 1860–1878.

Tomlinson, P. B. (2016). *The botany of mangroves* (2nd ed.). Cambridge University Press.

Trapnell, C., Roberts, A., Goff, L., Pertea, G., Kim, D., Kelley, D. R., Pimentel, H., Salzberg, S. L., Rinn, J. L., & Pachter, L. (2012). Differential gene and transcript expression analysis of RNA-seq experiments with TopHat and Cufflinks. *Nature Protocols*, *7*(3), 562–578.

Van de Peer, Y., Mizrachi, E., & Marchal, K. (2017). The evolutionary significance of polyploidy. *Nature Reviews Genetics*, *18*(7), 411–424.

Vogel, M. O., Moore, M., König, K., Pecher, P., Alsharafa, K., Lee, J., & Dietz, K.-J. (2014). Fast retrograde signaling in response to high light involves metabolite export, MITOGEN-ACTIVATED PROTEIN KINASE6, and AP2/ERF transcription factors in Arabidopsis. *The Plant Cell*, *26*(3), 1151–1165.

Wang, D., Zhang, Y., Zhang, Z., Zhu, J., & Yu, J. (2010). KaKs_Calculator 2.0: A toolkit incorporating gamma-series methods and sliding window strategies. *Genomics, Proteomics & Bioinformatics*, *8*(1), 77–80.

Wang, X., Gao, Y., Wu, X., Wen, X., Li, D., Zhou, H., Li, Z., Liu, B., Wei, J., Chen, F., Chen, F., Zhang, C., Zhang, L., & Xia, Y. (2021). High-quality evergreen azalea genome reveals tandem duplication-facilitated low-altitude adaptability and floral scent evolution. *Plant Biotechnology Journal*, *19*(12), 2544–2560.

Wang, Y., Tang, H., DeBarry, J. D., Tan, X., Li, J., Wang, X., Lee, T., Jin, H., Marler, B., Guo, H., Kissinger, J. C., & Paterson, A. H. (2012). MCScanX: A toolkit for detection and evolutionary analysis of gene synteny and collinearity. *Nucleic Acids Research*, *40*(7), e49.

Wisniewski, M., Norelli, J., & Artlip, T. (2015). Overexpression of a peach CBF gene in apple: A model for understanding the integration of growth, dormancy, and cold hardiness in woody plants. *Frontiers in Plant Science*, *6*, 85.

Xie, J., Li, Y., Liu, X., Zhao, Y., Li, B., Ingvarsson, P. K., & Zhanga, D. (2019). Evolutionary origins of pseudogenes and their association with regulatory sequences in plants. *Plant Cell*, *31*(3), 563–578.

Xie, W., Guo, Z., Wang, J., He, Z., Li, Y., Feng, X., Zhong, C., & Shi, S. (2022). Evolution of woody plants to the land-sea interface – The atypical genomic features of mangroves with atypical phenotypic adaptation. *Molecular Ecology*, *32*(6), 1351–1365.

Xu, S., Ding, Y., Sun, J., Zhang, Z., Wu, Z., Yang, T., Shen, F., & Xue, G. (2022). A high-quality genome assembly of *Jasminum sambac* provides insight into floral trait formation and Oleaceae genome evolution. *Molecular Ecology Resources*, *22*(2), 724–739.

Xu, S., Guo, Z., Feng, X., Shao, S., Yang, Y., Li, J., Zhong, C., He, Z., & Shi, S. (2023). Where whole-genome duplication is most beneficial: Adaptation of mangroves to a wide salinity range between land and sea. *Molecular Ecology*, *32*(2), 460–475.

Xu, S., He, Z., Guo, Z., Zhang, Z., Wyckoff, G. J., Greenberg, A., Wu, C.-I., & Shi, S. (2017). Genome-wide convergence during evolution of Mangroves from woody plants. *Molecular Biology and Evolution*, *34*(4), 1008–1015.

Yang, Z. (2007). PAML 4: Phylogenetic analysis by maximum likelihood. *Molecular Biology and Evolution*, *24*(8), 1586–1591.

Yu, G., Wang, L.-G., Han, Y., & He, Q.-Y. (2012). clusterProfiler: An R package for comparing biological themes among gene clusters. *OMICS: A Journal of Integrative Biology*, *16*(5), 284–287.

Yu, H., Yan, J., Du, X., & Hua, J. (2018). Overlapping and differential roles of plasma membrane calcium ATPases in Arabidopsis growth and environmental responses. *Journal of Experimental Botany*, *69*(10), 2693–2703.

Zachos, J. C., Dickens, G. R., & Zeebe, R. E. (2008). An early Cenozoic perspective on greenhouse warming and carbon-cycle dynamics. *Nature*, *451*(7176), 279–283.

Zhang, S., Liu, Y., Wang, B., Zhou, J., Yang, Y., Zhang, Y., & Liu, Q. (2023). Unraveling molecular mechanisms underlying low-temperature adaptation in *Laguncularia racemosa*. *Plant Physiology and Biochemistry*, *199*, 107747.

Zhang, Z., Carriero, N., Zheng, D., Karro, J., Harrison, P. M., & Gerstein, M. (2006). PseudoPipe: An automated pseudogene identification pipeline. *Bioinformatics*, *22*(12), 1437–1439.

Zhao, Q., Yang, D., Li, J., Bunting, P., Rosenqvist, A., Hilarides, L., Lucas, R. M., Thomas, N., Tadono, T., Worthington, T. A., Spalding, M., Murray, N. J., & Rebelo, L.-M. (2022). Global Mangrove Extent Change 1996–2020: Global Mangrove Watch Version 3.0. *Remote Sensing*, *14*, 3657.

Zheng, Y., Jiao, C., Sun, H., Rosli, H. G., Pombo, M. A., Zhang, P., Banf, M., Dai, X., Martin, G. B., Giovannoni, J. J., Zhao, P. X., Rhee, S. Y., & Fei, Z. (2016). iTAK: A program for genome-wide prediction and classification of plant transcription factors, transcriptional regulators, and protein kinases. *Molecular Plant*, *9*(12), 1667–1670.

Zhong, C., Li, S., Yang, Y., Zhang, Y., & Lin, Z. (2011). Analysis of the introduction effect of a mangrove species *Laguncularia racemosa*. *Journal of Fujian Forestry Science and Technology*, *8*(3), 96–99.

SUPPORTING INFORMATION

Additional supporting information can be found online in the Supporting Information section at the end of this article.

How to cite this article: Zhu, R., Shao, S., Xie, W., Guo, Z., He, Z., Li, Y., Wang, W., Zhong, C., Shi, S., & Xu, S. (2025). High-quality genome of a pioneer mangrove *Laguncularia racemosa* explains its advantages for intertidal zone reforestation. *Molecular Ecology Resources*, *25*, e13863. https://doi.org/10.1111/1755-0998.13863